Bull Earthquake Eng (2010) 8:519–534
DOI 10.1007/s10518-009-9110-0

ORIGINAL RESEARCH PAPER

Alternative interpretations of horizontal to vertical spectral ratios of ambient vibrations: new insights from theoretical modeling

Dario Albarello · Enrico Lunedei

Received: 20 December 2008 / Accepted: 15 March 2009 / Published online: 1 April 2009

Abstract Different positions exist about the physical interpretation of horizontal to vertical spectral ratios (HVSR) deduced from ambient vibrations. Two of them are considered here: one is based on the hypothesis that HVSR are mainly conditioned by body waves approaching vertically the free surface, the other one assumes that they are determined by surface waves (Rayleigh and Love, with relevant upper modes) only. These interpretations can be seen as useful approximations of the actual physical process, whose reliability should be checked case-by-case. To this purpose, a general model has been here developed where ambient vibrations are assumed to be the complete wave field generated by a random distribution of independent harmonic point sources acting at the surface of a flat stratified visco-elastic Earth. Performances of the approximate interpretations and complete wave field models have been evaluated by considering a simple theoretical subsoil configuration and an experimental setting where measured HVSR values were available. These analyses indicate that, at least as concerns the subsoil configurations here considered, the surface-waves approximation seems to produce reliable results for frequencies larger than the fundamental resonance frequency of the sedimentary layer. On the other hand, the body waves interpretation provides better results around the resonance frequency. It has been also demonstrated that the HVSR curve is sensitive to the presence of a source-free area around the receiver and that most energetic contribution of the body waves component comes from such local sources. This dependence from the sources distribution implies that, due to possible variations in human activities in the area where ambient vibrations are carried on, significant variations are expected to affect the experimental HVSR curve. Such variations, anyway, only weakly affect the location of HVSR maximum that confirms to be a robust indicator (in the range of 10%) of the local fundamental resonance frequency.

Keywords Ambient vibrations · HVSR · Geophysical modeling

D. Albarello (✉) · E. Lunedei
Dipatimento di Scienze della Terra, Università di Siena, Via Laterina 8, 53100 Siena, Italy
e-mail: albarello@unisi.it

E. Lunedei
e-mail: lunedei@unisi.it

1 Introduction

Ambient vibrations induced by both natural and anthropic sources are ubiquitous on the Earth surface and cover a large frequency interval (Peterson 1993). Under different denominations (microseisms, seismic noise, etc.) these vibrations have been explored since the beginning of modern seismology (e.g., Ferrari et al. 2000). However, in the recent years, the number of studies devoted to the analysis of ambient vibrations has undergone a dramatic increase (see, e.g., Bonnefoy-Claudet et al. 2006a): such a growing interest towards the characterization of seismic noise has been driven by the possibility to use such a small amplitude ground motion for cost effective seismic characterization of subsoil (e.g., D'Amico et al. 2008 and references therein) and the parameterization of building dynamical response (e.g., Wenzel and Pichler 2005). Among all, at least two international projects (EVG1-CT-2000-00026 SESAME, NATO-SfP980857) have been devoted to this argument. In the following some new results obtained in the frame of the last project are summarized.

The NATO Sfp980857 project focused on the development and application of fast and cost effective procedures for the study soil-structure interaction and vulnerability assessment in seismic areas. In this frame, most part of the work has been devoted to free-field and building vibration monitoring aiming at the seismic characterization of the local subsoil and parameterization of building dynamical properties. In particular, spectral ratios between free-field and building vibrations (Standard Spectral Ratios or SSR) have been considered to parameterize resonance properties of the buildings (see e.g., Parolai et al. 2005a; Gallipoli et al. 2008), while Horizontal to Vertical Spectral Ratios (HVSR) has been used to characterize resonance phenomena potentially responsible for the local enhancement of seismic ground motion (e.g., Nakamura 1989; Bard 1999; Mucciarelli and Gallipoli 2001).

HVSR have been extensively studied to detect the fundamental resonance frequency of a sedimentary cover (see, e.g., Haghshenas et al. 2008 and references therein) and retrieve information on the subsoil seismic layering (Arai and Tokimatsu 2004, 2005; Parolai et al. 2005b; Picozzi and Albarello 2007; Herak 2008). These last inversion procedures rely on two major competing hypotheses. On one side, Nakamura (2000) and Herak (2008) provide arguments supporting the idea that the HVSR curve is controlled by body waves. On the other side, it is suggested (e.g., Arai and Tokimatsu 2004, 2005; Lunedei and Albarello 2009a) that a major role is played by surface waves (both Rayleigh and Love phases with the relevant upper modes). Both models allows a correct interpretation of the HVSR maxima as representative of the fundamental resonance frequency of the sedimentary layer (Bard 1999) but provide divergent interpretations of the HVSR amplitudes. Of course, all the Authors are aware that both these positions represent approximations of the actual wave-field, that is expected to be a mixture of body and surface waves (e.g., Bonnefoy-Claudet et al. 2006a). On the other hand, such approximations are mandatory in order to set up a numerically feasible tool for the direct modeling of HVSR curves that can be implemented into an automatic inversion procedure (e.g., Picozzi and Albarello 2007, Herak 2008). Thus the open problem is the assessment of the respective reliability of these alternative interpretations in the frequency range of interest.

This problem has been intensely discussed in the frame of the project NATO Sfp project. To supply new arguments to this debate, implications of the above alternative interpretations of HVSR curve have been examined and compared with a new and more general physical representation of the ambient vibrations wave field, that allows to take into account both the contributions of body and surface waves. In order to evaluate the actual feasibility of these alternative models and in particular of approximate descriptions (body waves vs. surface waves) respective theoretical HVSR curves have been evaluated for each model in the case

of a simple subsoil configuration previously considered by Bonnefoy-Claudet et al. (2006b) and at an Italian test site where experimental HVSR data are available along with seismic parameters of the local subsoil.

2 Theoretical models of the HVSR curve deduced from ambient vibrations

In general, two aspects are of major concern in the study of HVSR from ambient vibrations. The first one is the definition of optimal experimental setting and post processing procedures to individuate features useful for practical purposes (see, e.g., Mucciarelli 1998; Picozzi et al. 2005; Chatelain et al. 2008). The second one concerns the physical interpretation and modeling of the ambient vibrations wave field. This is a fundamental pre-requisite to establish a link between observations and subsoil structure and thus using ambient vibrations to infer dynamical properties of the subsoil (Arai and Tokimatsu 2004, 2005; Parolai et al. 2005b; Picozzi and Albarello 2007; Herak 2008). On this topic, a strong debate has developed in the last years. Experimental studies (see the extensive review provided by Bonnefoy-Claudet et al. 2006a) provide a number important insights but remain inconclusive about some of important aspects, as discussed below. A good agreement exists about the fact that microseisms, i.e. low frequency ambient vibrations (< 0.5 Hz), are mainly associated to natural processes (oceanic waves, storms, etc.), while microtremors, i.e. high frequency ambient vibrations (> 1 Hz), are mainly associated to human activities. Both natural and anthropic sources contribute to vibrations in the intermediate frequency range. As a consequence of the possible strong variability of these sources at several time and space scales, ambient vibrations are considered an inherently stochastic phenomenon (e.g., Okada 2003). Thus, the possibility to exploit random vibrations for the seismic characterization of the subsoil relies on the availability of reliable models linking specific average aspects of environmental vibrations and subsoil seismic parameters. Experimental studies indicate that surface waves are present in the ambient vibrations wave field (e.g., Okada 2003) but provide contradictory results as concerns their relative importance with respect to body waves. Theoretical models relative to single sources (Tokimatsu 1997) and numerical simulations (Lachet and Bard 1994; Fäh et al. 2001; Bonnefoy-Claudet et al. 2006b; Bonnefoy-Claudet et al. 2008) provide more straightforward indications, suggesting that the role of surface waves at frequencies larger than the resonance frequency f_0 of the local subsoil become increasingly important when the seismic impedance contrast at sediment-bedrock interface increases. It also results that the Rayleigh waves contribution becomes progressively less important below the resonance frequency (Sherbaum et al. 2003). Furthermore, the location of ambient vibrations sources with respect to the receiver also affects the expected wave field. In particular, one can see that when source-receiver distances r are larger than the wavelength $\lambda_0 = V_S/f_0$, where V_S is the S waves velocity in the sedimentary cover, surface waves contribution become dominant. However, no convincing definitive result is provided about the respective role of body and surface waves around and below the resonance frequency. It is worth noting that this uncertainty does not affect the good correspondence between HVSR maxima and f_0, that has been well established on empirical basis (Haghshenas et al. 2008).

Nakamura (2000) provided some arguments supporting the idea that HVSR (at least as concerns its amplitude at the resonance frequency f_0) directly represents the response function for S waves ($F_S(f_0)$) at the top of a sedimentary layer overlying a rigid bedrock. In the case that both soil and bedrock are characterized by a weakly dissipative behavior, complex response function $F_\beta(f)$ (where f is the frequency) relative to the body waves phase

β (S of P) vertically propagating from depth can be computed numerically (e.g., Tsai 1970). In the hypothesis that the Nakamura (2000) model holds, one has

$$HVSR(f_0) = |F_S(f_0)| \ . \tag{1}$$

Herak (2008) generalizes this position by assuming that the ambient vibrations are constituted by body waves moving vertically. In this case, amplitudes of P and S phases respectively control vertical and horizontal ground motion components. If one also assumes that impinging P and S phases have the same amplitude in the bedrock, HVSR at the surface is determined by the respective amplifications of these phases induced by seismic properties of sedimentary layers overlying the bedrock. In this position, the HVSR curve can be modeled as the ratio between transfer functions relative to S waves (horizontal components) and P waves (vertical component):

$$HVSR(f) = \frac{|F_S(f)|}{|F_P(f)|} \ . \tag{2}$$

In both these models, no hypothesis is advanced about the sources responsible for the observed ambient vibrations and surface waves are considered to play a negligible role only. However, this assumption is not compatible with the fact that surface waves actually exist in the ambient vibrations wave field as ubiquitously revealed by experimental studies (e.g., Okada 2003). Furthermore, due to different attenuations relative to body and surface waves, it appears more plausible that most of active sources relatively distant from the sensor will provide a contribution in terms of surface waves larger that that of body waves.

By taking these aspects into account, a different interpretation has been proposed by several Authors (e.g., Fäh et al. 2001; Konno and Ohmachi 1998; Scherbaum et al. 2003) which is based on the hypothesis that surface waves play a major role in the definition of observed HVSR curves. The most general approach in this frame has been provided by Arai and Tokimatsu (2004, 2005) that takes into account both Rayleigh and Love waves (with the relevant upper modes) to model HVSR curves in the frame of a probabilistic approach. In this model, ambient vibrations are assumed to be constituted by plane waves randomly propagating in all the directions with different modes (Aki 1957). These are the result of the random activation of independent harmonic point forces applied at the surface of flat layered elastic Earth. The distribution of sources is assumed to be characterized by a uniform probability distribution all around the receiver. The plane waves constituting ambient vibrations are interpreted as surface waves (Rayleigh, Love and relative modes) and thus a link can be established between the seismic layering of the subsoil and expected average HVSR. This model has been recently generalized (Lunedei and Albarello 2009a) to include the effect of material damping in the case of weak dissipation (see the short outline of this formalization in Appendix A). It is worth noting that, since plane waves are considered only, sources taken into account in the model should be located sufficiently far away from the receiver to warrant that this assumption is realistic. This implies that a source-free area exists around the receiver. Several choices are possible about the dimension of this source-free area (e.g., Arai and Tokimatsu 2004; Lunedei and Albarello 2009a) and such choices significantly affect the expected HVSR curve. This dependence from a conventional position, represents a weak point of this modeling approach. Anyway, some dependence on the sources/receiver configuration cannot be ignored (see, e.g., Fäh et al. 2001; Bonnefoy-Claudet et al. 2006b; Bonnefoy-Claudet et al. 2008). Another problem concerns the effect of modal truncation. It is well known that strong seismic impedance contrasts increase the importance of surface waves upper modes in transferring seismic energy. Since propagation of these upper modes is conditioned by subsoil features at deeper depth with

respect to those affecting fundamental modes, their correct modeling requires the artificial introduction of deep layers in the model to avoid unrealistic truncations of such modes (see, e.g., Arai and Tokimatsu 2004, 2005). On the other hand, the characteristics of such deep layers are very poorly constrained by observations and this introduces a possible biases in the model.

Since it is well known (e.g., Bonnefoy-Claudet et al. 2006a) that both body waves and surface waves contribute to ambient vibrations, the above competing interpretations can be seen as useful approximations whose validity should be checked case by case. A possibility in this sense, at least as far as a flat visco-elastic layered Earth is considered, can be provided by modeling the complete wave field without any selection of the involved phases and avoiding as long as possible other approximations (e.g., Harkrider 1964; Aki and Richards 1980; Ben-Menahem and Singh 2000). This general approach is numerically troublesome and the solutions require numerical integrations which are very slow to converge when both the sources and the receiver are located at the same depth. This drawback is of major importance in simulating ambient vibrations, that are presumed to be generated by shallow sources and are revealed by sensors located on the surface (e.g., Bonnefoy-Claudet et al. 2006b). This problem has been solved by Hisada (1994) and its numerical code has been used by Bonnefoy-Claudet et al. (2006b, 2008) to simulate the effect of a distribution of independent random sources. This formalization has been generalized by Lunedei and Albarello (2009b) in the frame of a formally coherent probabilistic model. This model allows to compute average powers of ambient vibrations in the assumption that these are generated by random independent harmonic point sources distributed with uniform probability around the receiver and that subsoil is considered a flat layered visco-elastic medium. The basic elements of this generalization are shortly outlined in Appendix B. The resulting model is computationally feasible, despite of the relatively strong numerical efforts required to obtain stable solutions (run times are of the order of some hours on a standard personal computer). Despite of the fact that it is actually a theoretical model only, due to its generality it can be considered as a useful benchmark for checking the effectiveness of approximated interpretations discussed above in the situations of possible interest.

3 Comparison of theoretical HVSR deduced from approximate and complete wavefield models

Since body-waves (Eqs. 1, 2) and surface-waves (Appendix A) models represent alternative possible approximations of the actual ambient vibrations wave field, their feasibility in specialized situations has to be checked case by case. An example of this kind of assessment is described in the following and concerns the simple subsoil configuration in Table 1 (Bonnefoy-Claudet et al. 2006b). The S- and P-waves transfer functions $F_\beta(f)$ used to evaluate the expected HVSR curve implied by the Nakamura and Herak models (Eqs. 1 and 2, respectively) can be computed analytically in the form

$$F_\beta(f) = \left\{ \cos\left[2\pi f \frac{H}{V_{\beta,a}(2\pi f)}\right] + i \frac{\rho_a V_{\beta,a}(2\pi f)}{\rho_b V_{\beta,b}(2\pi f)} \sin\left[2\pi f \frac{H}{V_{\beta,a}(2\pi f)}\right] \right\}^{-1}, \quad (3)$$

where f is the frequency, H the thickness of the soft sedimentary layer, V_β the complex velocity of phase β and the indexes a and b respectively refer to the soft layer and bedrock (Kramer 1996). The complex velocity V_β accounts for material damping. If one expresses damping in terms of seismic quality factor Q_β of the body wave of concern, one has

Table 1 Seismic profile in Bonnefoy-Claudet *et al.* (2006b)

Thickness (m)	$V_P(m/s)$	$V_S(m/s)$	$\rho(kg/m^3)$	Q_P	Q_S
25	1, 350	200	1, 900	50	25
∞	2, 000	1, 000	2, 500	100	50

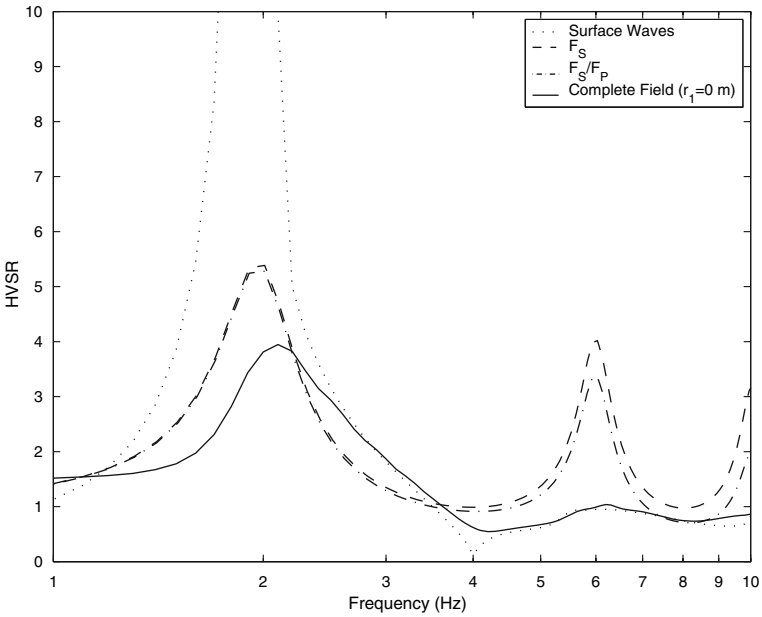

Fig. 1 Expected patterns of the V_S transfer function (F_S) and HVSR curves deduced for the subsoil configuration in Table 1, in the hypothesis of Herak (F_S/F_P), Lunedei and Albarello ("Surface waves") and that obtained by using the general probabilistic formulation in Appendix B ("Complete") in the hypothesis of a uniform distribution of sources all around the receiver ($r_1 = 0$ and $r_2 = 100$ km)

$$V_\beta(2\pi f) = \frac{V_\beta^e}{1 - \frac{1}{\pi Q_\beta} \log\left(\frac{f}{f_{\text{ref}}}\right)} \left(1 + i\frac{1}{2Q_\beta}\right), \tag{4}$$

where V_β^e is the elastic velocity of the body waves of concern (see values in Table 1) and f_{ref} is a reference frequency here considered equal to 1 Hz (Aki and Richards 1980). The S-waves response function is shown, by dashed line, in Fig. 1. In the hypothesis of Nakamura, its maximum should coincide with the observed HVSR maximum, according with Eq. 1. A very slight different pattern is obtained for the HVSR curve in the Herak hypothesis (Eq. 2). One can see (Fig. 1) that, at least as concerns the range of frequencies here considered, the two approaches show minor differences only. On the same plot, the theoretical H/V curve obtained by using the surface waves approximation described in Appendix A is also reported. As expected, in the presence of a sharp impedance contrast at the basis of the sedimentary layer (about 6.5), HVSR curve seems to be controlled by ellipticity of Rayleigh waves (Tokimatsu 1997; Konno and Ohmachi 1998). Since at f_0 vertical components of Rayleigh waves vanish both as concerns the fundamental and upper modes (e.g., Fäh et al. 2001), the expected HVSR curve shows a very large peak in correspondence of the resonance frequency (Fig. 1). It is worth noting that, as remarked by Nakamura (2000) this large peak appears at a frequency slightly different (1.9) from the actual value of f_0 (2 Hz). Such a difference

has been discussed by Malischewsky and Scherbaum (2004) on the basis of theoretical arguments and has been attributed to the properties of Rayleigh waves ellipticity (for a more general discussion about Rayleigh waves particle motion in simple subsoil configurations, see Malischewsky et al. 2008).

All these results have been compared with those obtained by using the more general model of the ambient vibrations wave field described in Appendix B. Due to its generality, this model has been here considered as a benchmark for the alternative approximate formulations. Resulting HVSR curve has been obtained by posing r_1 and r_2 respectively equal to 0 and 100 Km, and it is plotted with solid line in Fig. 1. It can bee seen that HVSR resulting from the more general model presents one peak only, near the S-waves resonance frequency f_0. It is worth noting that in this case, the HVSR maximum provides a slight overestimate of the resonance frequency (2.1 Hz vs. 2.0). A second major feature concerns the amplitude of the HVSR maximum, that results smaller than that computed by both the approximate models. One can also see that a fairly good agreement exists in the frequency range above f_0 (> 3 Hz) among the HVSR curves.

In order to better understand differences observed in Fig. 1, one should also take into account other differences among approximate and complete wave field models. An important aspect concerns the geometry of sources responsible for the ambient vibrations wave field. The distribution of sources and in particular their average distance from the receiver is recognized to significantly affect the shape of expected HVSR (e.g., Bonnefoy-Claudet et al. 2006b). The HVSR in the hypothesis that a dominant effect is played by vertically incident and resonant body waves are assumed to be independent from the distribution of sources. Instead, in the hypothesis that surface waves dominate ambient vibrations, HVSR strongly depends on the dimensions of a source-free area around the receiver (Lunedei and Albarello 2009a). In order to make more evident the effect of different configurations in the sources/receiver geometries, a new HVSR curve has been computed with the formulation of Appendix B by assuming a circular source-free area around the receiver with a radius of 100 m. The results of this new run are reported in Fig. 2 along with HVSR curves provided in the frame of surface waves interpretation. One can see that in this case, the correspondence between the HVSR curves obtained with the more general model and that deduced from surface waves only improves around the resonance frequency. Furthermore, one can see that the HVSR peak deduced from the general model increases with respect to the corresponding one in Fig. 1 and reaches values higher than those relative to the expected S-waves response function (F_S in Figs. 1 and 2). These results imply that HVSR curve (but as concerns a small interval around the resonance frequency f_0) resulting from the activity of relatively distant sources is essentially determined by surface waves polarization (both Love and Rayleigh) and this is true both above and below f_0.

4 Comparison of theoretical HVSR curves with observations at a test site

The considered site is located nearby the famous Pisa Leading Tower, one of the most important monuments of Italy. The site has been extensively studied in the past and noticeable efforts have been devoted for the geotechnical characterization of the Tower foundations (Jamiolowski and Pepe 2001 and references therein). A summary of available information is reported by Foti (2003). The subsoil is mainly constituted by succession of clayey and sandy silts at least up to 70 m from the ground level. Seismic measurements carried on by using a cross-hole configuration has provided V_S and V_P profiles at the site. Laboratory and in situ measurements have been used to characterize attenuation properties of the shallow

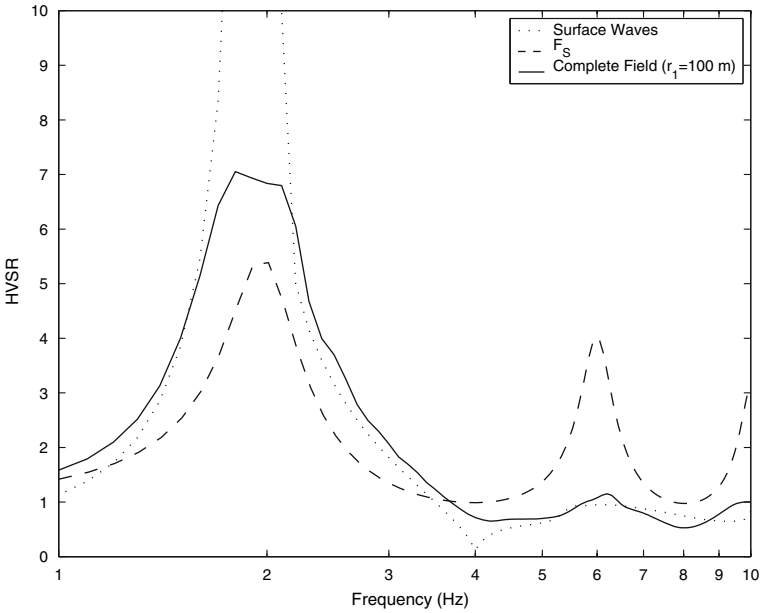

Fig. 2 Expected patterns of the S-waves transfer function (F_S) and HVSR values deduced for the subsoil configuration in Table 1 by the model in Appendix A ("Surface waves") and that obtained by using the more general probabilistic formulation in Appendix B ("Complete") with a source free area around the receiver ($r_1 = 100$ m and $r_2 = 100$ km)

subsoil. As concerns the laboratory test (Lo Presti et al. 1997), many high quality samples from the clayey layers in the depth range $12 \div 17$ m have been retrieved and tested. The damping ratio was evaluated during a series of cyclic torsional shear tests identifying values ranging between 2 and 3% in the very small strain range ($< 0.01\%$). These values remains nearly constant with frequency. Further in-situ information on the damping profile has been obtained from seismic tests (Foti 2003).

HVSR measurements have been carried on at a site located nearby (100 m apart) the Leading Tower, at the center of the City in a very crowd area. Tourists were walking near the sensors and an intense vehicular traffic took place all around the measurement area. Ambient vibrations measurements have been carried on by using the digital tromograph Tromino (www.tromino.it) and HVSR estimates have been obtained by following the procedure described in D'Amico et al. (2008) in line with indications provided by international agreements (see SESAME European project 2005). The resulting HVSR have been reported in Fig. 3 (solid line) and shows a clear maximum at the frequency of about 1.3 Hz with an amplitude of 2.4.

Theoretical HVSR curves have been computed for the Pisa test site by using the subsoil parameters in Table 2 that have been deduced from Foti (2003). The results of these computations carried on by considering the complete wave field model, the surface waves and body waves approximations (by following Lunedei and Albarello 2009a, b and Herak 2008) are reported in Fig. 3.

In general, all the theoretical HVSR curves mimic the overall shape of experimental HVSR with maximum values in the range $1 \div 2$ Hz and an amplitude in the range $2 \div 4$. However, significant differences also exist. To evaluate such differences on a quantitative basis, the overall misfit of each considered model has been computed in terms of standard deviation

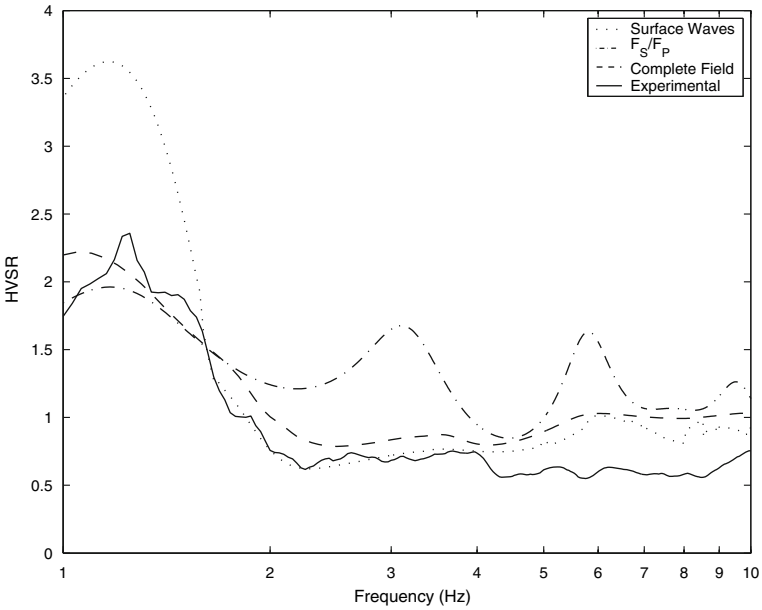

Fig. 3 Comparison of measured HVSR curve at the Pisa test site with patterns predicted by using different ambient vibrations models with the experimental subsoil configuration in Table 2. In particular, the theoretical HVSR curves deduced in the hypothesis of Herak (F_S/F_P) and of Lunedei and Albarello ("Surface waves") are considered along with the one obtained by using the general probabilistic formulation in Appendix B ("Complete Field") with $r_1 = 0$ and $r_2 = 100$ km

Table 2 Seismic profile of the subsoil at the Pisa test site derived from Foti (2003)

Thickness (m)	V_P (m/s)	V_S (m/s)	$\rho(kg/m^3)$	Q_P	Q_S
3	750	150	1, 600	10	10
2	1, 150	150	1, 600	10	10
3	1, 550	200	1, 600	18	18
4	1, 550	150	1, 900	18	18
9	1, 450	150	1, 900	18	18
8	1, 750	250	1, 700	25	25
11	1, 650	200	1, 700	25	25
9	1, 850	300	1, 700	25	25
3	2, 300	600	1, 700	25	25
∞	1, 900	400	1, 700	25	25

(squared root of the average squared residual) with respect to the experimental HVSR curve. As a whole, the worse result has been obtained by using the body waves approximation with a misfit value (0.57) much larger than that relative to surface waves approximation (0.40). As expected, the best fitting model results to be the one based on the complete wave field solution (0.32). This result corroborates the choice of the complete wave field model as a benchmark for other approximations.

However, beyond these general evaluations one can see that the comparison of the theoretical and experimental HSVR shapes confirms results deduced in the previous section. In particular, one can see that, in the frequency range above the resonance frequency (roughly estimated by the maximum of the observed HVSR), surface waves approximation provides

results that are better agreement with observations with respect to those provided by the body waves approximation. On the contrary, the amplitude of HVSR maximum is largely overestimated by the surface waves approximation and well reproduced by the body waves approximation.

5 Conclusions

A new general model has been presented to compute theoretical HVSR values of ambient vibrations at the surface of a weakly dissipative layered Earth. In this model, average spectral amplitudes of ambient vibrations have been modeled as the complete wave field generated at the surface of the Earth by a uniform distributions of independent point-like harmonic sources. Due to its generality, this model can be considered a benchmark for approximate alternative models that requires less computational efforts with respect to the general model here presented. In particular, two alternative models have been considered, that are based on the assumption that ambient vibrations are controlled by body waves and surface waves respectively. To evaluate the feasibility of this new model and the major differences with results provided by the alternative approximate models, two subsoil configurations have been considered. In the first case, a purely theoretical setting has been examined. In the second case, complete and approximate models have been used to compute theoretical HVSR curves at a test site in Italy where experimental HVSR data were available along with data concerning seismic parameters of the local subsoil. In general, the two applications provide similar results.

In particular, it results that the maximum of the expected HVSR curve is a robust estimator (within a range of about 10%) of the fundamental resonance frequency of the sedimentary cover f_0. On the other hand, in line with results of previous experimental and theoretical studies (e.g., Haghshenas et al. 2008), it has been seen that HVSR amplitudes (whatsoever the underlying model is) at the resonance frequency both underestimate and overestimate the actual response function relative to S-waves. Furthermore, the present study corroborates and generalizes findings provided by previous analyses (Tokimatsu 1997; Bonnefoy-Claudet et al. 2006b) as concerns the dominance of surface waves for ambient vibrations at frequencies larger than f_0. Apparently, at least for the specific subsoil configurations here considered, the body waves model fails to reproduce the HVSR amplitudes but as concerns a small interval around f_0 where the amplitude of Rayleigh waves vanishes. In this frequency domain, there is a fair correspondence between HVSR amplitudes provided by body waves approximation and that deduced from the more general model. This suggests that body waves probably play a significant role only in a limited (whether very important for practical purposes) frequency band. This suggests that a more effective inversion procedure should possibly consider both body waves and surface waves approximation, each relative to a different frequency band (around and above f_0 respectively).

Another important consequence of the results here obtained, is the fact that the shape of the HVSR curve around f_0, strongly depends on the radius of the source free area around the receiver. This is a basic point for practical measurements of HVSR from ambient vibrations. A direct implication is that at the same site, different HVSR shapes around f_0 (and markedly different maximum amplitudes) can be the effect of different distributions of human activities around the receiver up to distances of the order of hundreds meters. In general, in many cases (e.g., in urban areas), it is not possible to evaluate the minimum distance of sources responsible for observed ambient vibrations neither its eventual variations in time.

This implies that no firm conclusion can be drawn from the inversion of HVSR shape around and below the resonance frequency.

Acknowledgements Many thanks are due to the two anonymous Referees, whose comments and suggestions helped us to improve the manuscript. The authors also thank Prof. Marijan Herak, who kindly supplied the numerical code for the computation of S-waves response function in a weakly dissipative layered Earth. This work has been developed with financial support of the NATO Sfp980857 Research Project.

Appendix A

Aki (1957) describes ambient vibrations as a stochastic wave field constituted by a linear combination of independent harmonic plane waves with aleatory amplitudes, propagating in all directions on the Earth surface. The waves are assumed to be dispersive and multimodal, in that multiple phase velocities are allowed for each frequency. Arai and Tokimatsu (2004) have interpreted such plane waves as surface waves generated by a continuous distribution of independent harmonic point-like sources with stochastic amplitudes located at the surface of a flat layered elastic Earth. The same model has been generalized by Lunedei and Albarello (2009a) to include the effect of weak material damping. In this situation, any correlation between the average spectral amplitudes of propagation modes is lost and thus, the average spectral power relative to each mode can be computed by separately combining the relevant Love and Rayleigh contributions generated by a generic source. This contribution in terms of power spectral density $P_n(\omega)$ relative to the angular frequency ω has the form

$$P_n(\omega) = \int M\left[|A_n(\omega; r, \phi)|^2\right] r \, d\phi \, dr \,, \tag{5}$$

where the integrand represents the average contribution to the $n-$th surface waves propagation mode of sources located in a unitary surface element at a distance r and azimuth ϕ with respect to the receiver. The bulk of the model is the evaluation of the above integrand as a function of the average spectral power of harmonic sources active in the unitary area, position and average orientation of sources in the relevant area and the seismic layering of the subsoil.

To evaluate the spectral amplitudes in Eq. 5 in the case that sources are sufficiently far away from the receiver that surface waves dominate the wave field, the contribution of single harmonic sources in the unitary surface element has to be computed. It results (Aki and Richards 1980; Ben-Menahem and Singh 2000; Lai and Rix 2002) that, if a generic point-like source in the form $\mathbf{F}(t) \equiv \left(F_x, F_y, F_z\right) \cdot e^{-i\omega t}$ is assumed, ground motion spectral amplitudes at the receiver relative to Love and Rayleigh phases in the visco-elastic domain result to be

$$\left[A_{L,n}(\omega; r, \phi)\right]_{\hat{\boldsymbol{\phi}}} = \frac{F_x \sin\phi - F_y \cos\phi}{4\sqrt{2\pi\omega r}} \cdot e^{-\alpha_{L,n} r} \cdot B_{0,n} \tag{6}$$

$$\left[A_{R,n}(\omega; r, \phi)\right]_{\hat{\boldsymbol{r}}} = -\frac{e^{-\alpha_{R,n} r}}{4\sqrt{2\pi\omega r}} \cdot \left[i \cdot F_z \cdot B_{3,n} - \left(F_x \cos\phi + F_y \sin\phi\right) \cdot B_{1,n}\right] \tag{7}$$

$$\left[A_{R,n}(\omega; r, \phi)\right]_{\hat{\boldsymbol{z}}} = \frac{e^{-\alpha_{R,n} r}}{4\sqrt{2\pi\omega r}} \cdot \left[F_z \cdot B_{2,n} - i \cdot \left(F_x \cos\phi + F_y \sin\phi\right) \cdot B_{3,n}\right] \,, \tag{8}$$

where $B_{j,n}$, for $j = 0, 1, 2, 3$, contains the Love or Rayleigh phase and group velocities and the eigenfunctions of the $n-$th mode, wile $\alpha_{\beta,n}$ is the attenuation coefficient of the $n-$th mode of the $\beta-$kind wave (see Lunedei and Albarello 2009a for more details).

Being $N_L(\omega)$ and $N_R(\omega)$ the number of active Love and Rayleigh modes respectively, ambient vibrations result from the superposition of $N_L(\omega)+2N_R(\omega)$ uncorrelated stochastic wave fields. The average spectral power of each of these fields can be computed from the average of the squared amplitudes (6÷8). A continuous distribution of sources is assumed to exist on an appropriate region of the Earth surface, $\mathcal{C}(r_1) \equiv \left\{(x, y) \in \mathbb{R}^2 \;\middle|\; x^2 + y^2 \geq r_1^2\right\}$, which excludes the circle with radius $r_1 \geq 0$. This last area is considered to be source-free in order to warrant the dominance of surface waves and the validity of the plane-waves approximation. In this view, the average power of sources active in the unitary surface element in the principal directions is $\sigma^2\sigma_i^2$ $(i = x, y, z)$: σ_i are the cosine directors (*ergo* $\sigma_x^2 + \sigma_y^2 + \sigma_z^2 = 1$).

With this position, the power contribution of each mode can be written in the form (Lunedei and Albarello 2009a)

$$P_{HL,n}(\omega) \equiv \int_{\mathcal{C}(R_1)} M\left[A_{L,n}(\omega; r, \phi)\right]_{\hat{\phi}}^2 \cdot r \, d\phi \, dr$$
$$= \frac{\sigma^2}{32\omega} \cdot \left|B_{0,n}\right|^2 \cdot \left(\sigma_x^2 + \sigma_y^2\right) \cdot \frac{e^{-2\alpha_{L,n} r_1}}{2\alpha_{L,n}} \tag{9}$$

$$P_{HR,n}(\omega) = \frac{\sigma^2}{32\omega} \cdot \left\{2\sigma_z^2 \cdot \left|B_{3,n}\right|^2 + \left(\sigma_x^2 + \sigma_y^2\right) \cdot \left|B_{1,n}\right|^2\right\} \cdot \frac{e^{-2\alpha_{R,n} r_1}}{2\alpha_{R,n}} \tag{10}$$

$$P_{VR,n}(\omega) = \frac{\sigma^2}{32\omega} \cdot \left\{2\sigma_z^2 \cdot \left|B_{2,n}\right|^2 + \left(\sigma_x^2 + \sigma_y^2\right) \cdot \left|B_{3,n}\right|^2\right\} \cdot \frac{e^{-2\alpha_{R,n} r_1}}{2\alpha_{R,n}} \tag{11}$$

(notice the dependence on the choice of the inner radius r_1).

On this basis, the effective velocities for the Love and Rayleigh components of the ambient vibrations, according to Arai and Tokimatsu, have the form

$$\left[\hat{V}_L(\omega)\right]_{\hat{\phi}} = \frac{\omega \cdot \xi}{\arccos\left[\sum_n \frac{P_{HL,n}(\omega)}{P_{HL}(\omega)} \cdot \cos\left(\frac{\omega}{\Re V_{L,n}(\omega)} \cdot \xi\right)\right]} \tag{12}$$

$$\left[\hat{V}_R(\omega)\right]_{\hat{r}} = \frac{\omega \cdot \xi}{\arccos\left[\sum_n \frac{P_{HR,n}(\omega)}{P_{HR}(\omega)} \cdot \cos\left(\frac{\omega}{\Re V_{R,n}(\omega)} \cdot \xi\right)\right]} \tag{13}$$

$$\left[\hat{V}_R(\omega)\right]_{\hat{z}} \equiv \frac{\omega \cdot \xi}{\arccos\left[\sum_n \frac{P_{VR,n}(\omega)}{P_{VR}(\omega)} \cdot \cos\left(\frac{\omega}{\Re V_{R,n}(\omega)} \cdot \xi\right)\right]}, \tag{14}$$

where $P_\bullet(\omega) \equiv \sum_n P_{\bullet,n}(\omega)$.

The corresponding expected HVSR curve results from the expression

$$HVSR(\omega) \equiv \sqrt{\frac{P_H(\omega)}{P_V(\omega)}}, \tag{15}$$

where

$$P_H(\omega) \equiv \sqrt{\left[\sum_{n=1}^{N_L(\omega)} P_{HL,n}(\omega)\right] \cdot \left[\sum_{n=1}^{N_R(\omega)} P_{HR,n}(\omega)\right]} \tag{16}$$

$$P_V(\omega) \equiv \sum_{n=1}^{N_R(\omega)} P_{VR,n}(\omega). \tag{17}$$

It is worth noting that the effective velocities and HVSR only depend on the relative ratios among the source power along the different directions: in other words, cosine directors σ_i are of concern only.

Appendix B

In the same approximations in Appendix A, the general solution of the wave motion equation relative to a stratified medium (see, e.g., formula (11) of Hisada 1994) has been considered. Here, displacements are given as the combination of a number of integrals of Bessel functions times some coefficients (which are called Hs and Vs in the Hisada's formalization) and are linear functions of the source components (see, e.g., Lamb 1904; Harkrider 1964; Tokimatsu 1997). As shown in Lunedei and Albarello (2009b) the displacements at origin (where the receiver is located) can be defined as

$$u_r(r,\vartheta) = \tilde{u}_r(r)\cdot\left(F_x\cdot\cos\vartheta + F_y\cdot\sin\vartheta\right) + u_r^*(r)\cdot F_z \tag{18}$$

$$u_\vartheta(r,\vartheta) = \tilde{u}_\vartheta(r)\cdot\left(-F_y\cdot\cos\vartheta + F_x\cdot\sin\vartheta\right) \tag{19}$$

$$u_z(r,\vartheta) = \tilde{u}_z(r)\cdot\left(F_x\cdot\cos\vartheta + F_y\cdot\sin\vartheta\right) + u_z^*(r)\cdot F_z, \tag{20}$$

where

$$\tilde{u}_r(r) \equiv -\int_0^{+\infty}\left\{R_{1,H}(k)\cdot\frac{dJ_1(kr)}{d(kr)} + L_H(k)\cdot\frac{J_1(kr)}{kr}\right\}dk \tag{21}$$

$$u_r^*(r) \equiv -\int_0^{+\infty}\left\{R_{1,V}(k)\cdot J_1(kr)\right\}dk \tag{22}$$

$$\tilde{u}_\vartheta(r) \equiv \int_0^{+\infty}\left\{R_{1,H}(k)\cdot\frac{J_1(kr)}{kr} + L_H(k)\cdot\frac{dJ_1(kr)}{d(kr)}\right\}dk \tag{23}$$

$$\tilde{u}_z(r) \equiv \int_0^{+\infty}\left\{R_{2,H}(k)\cdot J_1(kr)\right\}dk \tag{24}$$

$$u_z^*(r) \equiv -\int_0^{+\infty}\left\{R_{2,V}(k)\cdot J_0(kr)\right\}dk. \tag{25}$$

The coefficients of the Bessel functions are

$$\begin{aligned} L_H(k) &\equiv H_{1\ell}^1(0;0)/F_\ell \\ R_{1,H}(k) &\equiv V_{1\ell}^1(0;0)/F_\ell, \\ R_{2,H}(k) &\equiv V_{2\ell}^1(0;0)/F_\ell \end{aligned}$$

for $\ell = x$ or $\ell = y$ (it is the same, since the linearity in the source components), and

$$\begin{aligned} R_{1,V}(k) &\equiv V_{1z}^1(0;0)/F_z \\ R_{2,V}(k) &\equiv V_{2z}^1(0;0)/F_z, \end{aligned}$$

where the Hs and Vs functions are given by Hisada (1994). Then, a ring $\mathcal{C}(r_1, r_2) \equiv \left\{(x, y) \in \mathbb{R}^2 \;\middle|\; r_1 \leq \sqrt{x^2 + y^2} \leq r_2\right\}$ is considered that is uniformly filled by independent random sources with average power density (the average squared amplitude) in the same form of Appendix A. Square amplitude of $u_j(r, \vartheta)$, for $j = r, \vartheta, z$, integrated on $\mathcal{C}(r_1, r_2)$ can be obtained by a little algebra, as shown in Lunedei and Albarello (2009b). By passing to a Cartesian frame, these variances are the total power components along the pricipal directions at the origin

$$\mathcal{V}_x^{TOT}(\omega) = \pi\sigma^2 \left\{ \frac{3}{4}\sigma_x^2 \int_{r_1}^{r_2} \left[|\tilde{u}_r(r)|^2 + |\tilde{u}_\vartheta(r)|^2 \right] r \, dr \right.$$
$$-\frac{1}{2}\sigma_x^2 \int_{r_1}^{r_2} \left\{ \Re\left[\tilde{u}_r(r)\right] \Re\left[\tilde{u}_\vartheta(r)\right] + \Im\left[\tilde{u}_r(r)\right] \Im\left[\tilde{u}_\vartheta(r)\right] \right\} r \, dr$$
$$\left. +\frac{1}{4}\sigma_y^2 \int_{r_1}^{r_2} |\tilde{u}_r(r) + \tilde{u}_\vartheta(r)|^2 \, r \, dr + \sigma_z^2 \int_{r_1}^{r_2} \left|u_r^*(r)\right|^2 r \, dr \right\}, \tag{26}$$

$$\mathcal{V}_y^{TOT}(\omega) = \pi\sigma^2 \left\{ \frac{1}{4}\sigma_x^2 \int_{r_1}^{r_2} |\tilde{u}_r(r) + \tilde{u}_\vartheta(r)|^2 \, r \, dr + \frac{3}{4}\sigma_y^2 \int_{r_1}^{r_2} \left[|\tilde{u}_r(r)|^2 + |\tilde{u}_\vartheta(r)|^2 \right] r \, dr \right.$$
$$\left. -\frac{1}{2}\sigma_y^2 \int_{r_1}^{r_2} \left\{ \Re\left[\tilde{u}_r(r)\right] \Re\left[\tilde{u}_\vartheta(r)\right] + \Im\left[\tilde{u}_r(r)\right] \Im\left[\tilde{u}_\vartheta(r)\right] \right\} r \, dr \right\}$$
$$\left. +\sigma_z^2 \int_{r_1}^{r_2} \left|u_r^*(r)\right|^2 r \, dr \right\}, \tag{27}$$

$$\mathcal{V}_z^{TOT}(\omega) = \pi\sigma^2 \int_{r_1}^{r_2} \left\{ |\tilde{u}_z(r)|^2 \left(\sigma_x^2 + \sigma_y^2\right) + 2\left|u_z^*(r)\right|^2 \sigma_z^2 \right\} r \, dr; \tag{28}$$

we remark that these quantities depend on ω, because the integrands are so.

These integrals require to be evaluated numerically, so it is necessary to set two suitable values for r_1 and r_2. Unlike the case described in Appendix A, no more physical constraint prevents from putting $r_1 = 0$, while r_2 has to be chosen case by case on the numerical estimate of the integrals convergence. After computing integrals, HVSR is given by formula (15), where

$$P_H(\omega) \equiv \sqrt{\mathcal{V}_x^{TOT}(\omega) \cdot \mathcal{V}_y^{TOT}(\omega)} \tag{29}$$
$$P_V(\omega) \equiv \mathcal{V}_z^{TOT}(\omega) \, . \tag{30}$$

In this case also, the HVSR only depends on the average power of source components σ_i $(i = x, y, z)$.

References

Aki K (1957) Space and time spectra of stationary stochastic waves, with special reference to microtremors. Bull Earthq Res Inst XXXV(3):415–457

Aki K, Richards PG (1980) Quantitative seismology—theory and methods, vol I. Freeman Company, San Francisco (USA)

Arai H, Tokimatsu K (2004) S-wave velocity profiling by inversion of microtremor H/V spectrum. Bull Seism Soc Am 94(1):53–63

Arai H, Tokimatsu K (2005) S-wave velocity profiling by joint inversion of microtremor dispersion curve and horizontal-to-vertical (H/V) spectrum. Bull Seism Soc Am 95(5):1766–1778

Bard P-Y (1999) Microtremor measurements: a tool for site effect estimation? In: Irikura K, Kudo K, Okada H, Sasatani T (eds) The effects of surface geology on seismic motion. Balkema, Rotterdam, pp 1251–1279

Ben-Menahem A, Singh SJ (2000) Seismic waves and sources. Dover Publications Inc, New York 1102

Bonnefoy-Claudet S, Cotton F, Bard P-Y (2006a) The nature of noise wavefield and its applications for site effects studies: a literature review. Earth Sci Rev 9(2006):205–227

Bonnefoy-Claudet S, Cornou C, Bard P-Y, Cotton F, Moczo P, Kristek J, Fäh D (2006b) H/V ratios: a tool for site effects evaluation. Results from 1-D noise simulations. Geoph J Int 167:827–837

Bonnefoy-Claudet S, Köhler A, Cornou C, Wathelet M, Bard P-Y (2008) Effects of love waves on microtremor H/V ratio. Bull Seism Soc Am 98(1):288–300

Chatelain J-L, Guillier B, Cara F, Duval A-M, Atakan K, Bard P-Y, The WP02 SESAME team (2008) Evaluation of the influence of experimental conditions on H/V results from ambient noise recordings. Bull Earthq Eng 6:33–74

D'Amico V, Picozzi M, Baliva F, Albarello D (2008) Ambient noise measurements for preliminary site-effects characterization in the urban area of florence. Bull Seism Soc Am 98(3):1373–1388. doi:10.1785/0120070231

Fäh D, Kind F, Giardini D (2001) A theoretical investigation of average H/V ratios. Geoph J Int 145:535–549

Ferrari G, Albarello D, Martinelli G (2000) Tromometric measurements as a tool for crustal deformation monitoring. Seism Res Lett 71(5):562–569

Foti S (2003) Small-strain stiffness and damping ratio of Pisa clay from surface wave test. Geotechnique 53:455–461

Gallipoli MR, Mucciarelli M, Vona M (2008) Empirical estimate of fundamental frequencies and damping for Italian buildings. Earthq Eng Struct Dyn (in press)

Haghshenas E, Bard P-Y, Theodulis N, SESAME WP04 Team (2008) Empirical evaluation of microtremor H/V spectral ratio. Bull Earthq Eng 6:75–108

Harkrider DG (1964) Surface waves in multilayered elastic media, part 1. Bull Seism Soc Am 54(2):627–679

Herak M (2008) ModelHVSR—a Matlab tool to model horizontal-to-vertical spectral ratio of ambient noise. Comp Geosci 34:1514–1526

Hisada Y (1994) An efficient method for computing green's functions for a layered half-space with sources and receivers at close depths. Bull Seism Soc Am 84(5):1456–1472

Jamiolowski M, Pepe MC (2001) Vertical yield stress for Pisa clay from piezocone tests. J Geotech Geoenv Eng ASCE 127:893–897

Konno K, Ohmachi T (1998) Ground-motion characteristics estimated from spectral ratio between Horizontal and Vertical components of microtremor. Bull Seism Soc Am 88(1):228–241

Kramer SL (1996) Geotechnical earthquake engineering. Prentice Hall, New Jersey 653

Lachet C, Bard P-Y (1994) Numerical and theoretical investigations on the possibilities and limitations of Nakamura's technique. J Geophys Earth 42:377–397

Lamb H (1904) On the propagation of tremors over the surface of an elastic solid. Phil Trans R Soc Lond A 203:1–42

Lai CG, Rix GJ (2002) Solution of the Rayleigh eigen problem in viscoelastic media. Bull Seism Soc Am 92(6):2297–2309

Lo Presti DCF, Pallaro O, Cavallaro A, (1997) Damping ratio of soils from laboratory and in-situ tests. In: Proceedings of the 14th international conference on soil mechanics and fundamental engineering, pp 391–400

Lunedei E, Albarello D (2009a) On the seismic noise wave field in a weakly dissipative layered earth. Geophys J Int (in press)

Lunedei E, Albarello D (2009b) Theoretical HVSR curves from the complete wave field modelling of ambient vibrations in a weakly dissipative layered earth. Geophys J Int (submitted)

Malischewsky PG, Scherbaum F (2004) Love's formula and H/V-ratio (ellipticity) of Rayleigh waves. Wave Motion 40:57–67

Malischewsky PG, Scherbaum F, Lomnitz C, Thanh Tuan T, Wuttke F, Shamir G (2008) The domain of existence of prograde Rayleigh-wave particle motion for simple models. Wave Motion 45:556–564

Mucciarelli M (1998) Reliability and applicability of Nakamura's technique using microtremors: an experimental approach. J Earthq Eng 2:625–638

Mucciarelli M, Gallipoli MR (2001) A critical review of 10 years of microtremor HVSR technique. Boll Geof Teor Appl 42:255–266

Nakamura Y (1989) A method for dynamic characteristics estimation of subsurface using microtremor on the ground surface. QR of RTRI 30(1):25–33

Nakamura Y (2000) Clear identification of fundamental idea of Nakamura's technique and its applications. In: Proceedings of the 12th world conference on earthquake engineering. Auckland, New Zealand, paper 2656

Okada H (2003) The microtremor survey method. In: Geophysical monograph series 12. Society of Exploration Geophysicists, 135 pp

Parolai S, Facke A, Richwalski SM, Stempniewski L (2005a) Assessing the vibrational frequencies of the Holweide hospital in the city of Cologne (Germany) by means of ambient seismic noise analysis and FE modelling. Natural Hazard 34:217–230

Parolai S, Picozzi M, Richwalski SM, Milkereit C (2005b) Joint inversion of phase velocity dispersion and H/V ratio curves from seismic noise recordings using a genetic algorithm, considering higher modes. Geophys Res Lett 32. doi:10.1029/2004GL021115

Peterson J (1993) Observation and modeling of background seismic noise. US Geol Survey, open file report. Albuquerque, pp 93–322

Picozzi M, Albarello D (2007) Combining genetic and linearized algorithms for a two-step joint inversion of Rayleigh wave dispersion and H/V spectral ratio curves. Geoph J Int 169:189–200

Picozzi M, Parolai S, Albarello D (2005) Statistical analysis of noise horizontal-to-vertical spectral ratios (HVSR). Bull Seism Soc Am 95(5):1779–1786. doi:10.1785/0120040152

Scherbaum F, Hinzen K-G, Ohrnberger M (2003) Determination of shallow shear wave velocity profiles in the Cologne, Germany area using ambient vibrations. Geoph J Int 152:597–612

Site Effects Assessment using Ambient Excitations (SESAME) European project (2005) Deliverable D23.12, Guidelines for the implementation of the H/V spectral ratio technique on ambient vibrations: measurements, processing and interpretation, http://sesame-fp5.obs.ujf-grenoble.fr/SESTechnicalDoc.htm. Accessed March 2008

Tokimatsu K (1997) Geotechnical site characterization using surface waves. In: Proceedings of the 1st international conference on earthquake geotechnical engineering, vol 3, pp 1333–1368

Tsai NC (1970) A note on the steady-state response of an elastic half-space. Bull Seism Soc Am 60:795–808

Wenzel H, Pichler D (2005) Ambient vibration monitoring. Wiley, The Atrium, Southern Gate, Chichester, West Sussex, England (UK), 291 pp